

LncRNA expression in the spinal cord modulated by minocycline in a mouse model of spared nerve injury

Zihao Liu
Ying Liang
Honghua Wang
Zhenhe Lu
Jinsheng Chen
Qiaodong Huang
Lei Sheng
Yinghong Ma
Huiying Du
Qingjuan Gong

Department of Pain Medicine,
The Second Affiliated Hospital of
Guangzhou Medical University,
Guangzhou, China

Abstract: Neuropathic pain is a common and refractory chronic pain that affects millions of people worldwide. Its underlying mechanisms are still unclear, but they may involve long non-coding RNAs (lncRNAs), which play crucial roles in a variety of biological functions, including nociception. We used microarrays to investigate the possible interactions between lncRNAs and neuropathic pain and identified 22,213 lncRNAs and 19,528 mRNAs in the spinal cord in a mouse model of spared nerve injury (SNI)-induced neuropathic pain. The abundance levels of 183 lncRNAs and 102 mRNAs were significantly modulated by both SNI and administration of minocycline. A quantitative real-time polymerase chain reaction analysis validated expression changes in three lncRNAs (*NR_015491*, *ENSMUST00000174263*, and *ENSMUST00000146263*). Class distribution analysis of differentially expressed lncRNAs revealed intergenic lncRNAs as the largest category. Functional analysis indicated that SNI-induced gene regulations might be involved in the activities of cytokines (IL17A and IL17F) and chemokines (CCL2, CCL5, and CCL7), whereas minocycline might exert a pain-alleviating effect on mice through actin binding, thereby regulating nociception by controlling the cytoskeleton. Thus, lncRNAs might be responsible for SNI-induced neuropathic pain and the attenuation caused by minocycline. Our study could implicate lncRNAs as potential targets for future treatment of neuropathic pain.

Keywords: lncRNA, neuropathic pain, spinal cord, minocycline

Introduction

Neuropathic pain is one of the most common and disabling causes of the chronic pain state, affecting up to 8% of the global population.¹ Defined as “pain caused by a lesion or disease of the somatosensory system”,² neuropathic pain may have a diverse array of clinical causes in both the peripheral and the central nervous system (CNS).¹ A substantial body of evidence points to several important aberrant pathogeneses that may contribute to neuropathic pain, such as peripheral and central sensitization^{3,4} and pathological activation of microglia.⁵⁻⁷ However, little is known about the genetic basis of the mechanisms behind these changes.

Human protein-coding genes represent only ~1%–2% of the genetic material or 25,000 genes.⁸ This indicates that most eukaryotic genomes are transcribed, but they generate a large population of noncoding RNAs (ncRNAs).⁹ Based on transcript size, these ncRNAs can be divided into small noncoding RNAs (<200 bp) and long noncoding RNAs (lncRNAs; ≥200 nt). Unlike the well-characterized microRNAs, the majority of small ncRNAs, lncRNAs are often poorly conserved at the sequence level and are considered to be subject to post-transcriptional processing, intracellular or intercellular transport, association

Correspondence: Qingjuan Gong
Department of Pain Medicine, The
Second Affiliated Hospital of Guangzhou
Medical University, 250 Changgang Road
East, Guangzhou 510260, China
Tel +86 20 3415 2379
Email gqj01@sohu.com

with RNA-binding proteins, and myriad interactions with other molecules.¹⁰ Therefore, lncRNAs can serve as highly dynamic, modular, multimodal, and energy efficient factors for epigenetic interference within the nucleus and cytoplasm.¹¹

Recent studies have shown that some lncRNAs are preferentially expressed in the nervous system when compared with other organ systems^{10,12,13} and that lncRNAs play important roles in diseases like neuropathic pain. For example, Jiang et al have reported a large number of differentially expressed (DE) lncRNAs in the spinal cord following spinal nerve ligation.¹⁴ A novel antisense lncRNA, *Kcna2*, which is also found in dorsal root ganglia (DRG), is thought to participate in the development of neuropathic pain by specifically silencing expression of *Kcna2* (which encodes the potassium voltage-gated channel subfamily A member 2).¹⁵ Two functional lncRNAs, *uc.48+* and *NONRATT021972*, regulate diabetic neuropathic pain (DNP) through the P2X₃ and P2X₇ receptors, respectively, in the DRG.^{16–18} These findings suggest that lncRNAs have an important effect on neuropathic pain.

One treatment for neuropathic pain is minocycline, a second-generation tetracycline antibiotic. This lipophilic molecule is absorbed rapidly and readily across the blood–brain barrier and may act by several possible mechanisms,^{19,20} including inhibition of immune cell and microglia activation, inhibition of proinflammatory cytokine release, inhibition of nitric oxide release, and augmentation of anti-inflammatory cytokine release. However, recent studies^{19,21} have addressed different opinions about the efficacy and the targets being inhibited. Unlike classic medications, such as gabapentin and pregabalin, that have well-known mechanisms operating generally at the protein level, the mechanism by which minocycline attenuates neuropathic pain is still unclear.¹⁹ In the present study, we investigated the genome-wide expression of lncRNAs and mRNAs in the spinal cord following spared nerve injury (SNI)-induced neuropathic pain, in an attempt to clarify the gene mechanisms underlying the pathophysiological aberrations that lead to neuropathic pain. We also used minocycline as a treatment control to filter genes that may be DE during the regulation of neuropathic pain, as well as to explore the mechanism of this drug at the gene level. The findings indicate that lncRNAs may represent crucial mediators and potential therapeutic targets for neuropathic pain.

Materials and methods

Animals

All experimental procedures were approved by the Institutional Animal Care and Use Committee of Guangzhou

Medical University and were carried out in accordance with the guidelines of the National Institutes of Health on animal care and the ethical guidelines for investigation of experimental pain in conscious animals.⁴⁴ Male Balb/c mice aged 8 weeks were purchased from Guangdong Medical Laboratory Animal Center (Guangzhou, China). Mice were housed in separated cages and the rooms were kept at 24±1°C (297±1 K) temperature and 50%–60% humidity, under a 12:12 light–dark cycle and with free access to food and water ad libitum. They were numbered and randomly allocated in 3 groups: Sham, vehicle (V)-SNI (vehicle repeatedly administered before and after SNI), and minocycline (MC)-SNI (minocycline repeatedly administered before and after SNI).

Behavioral tests

Mice of 3 groups (6 per group) were tested for basal paw withdrawal mechanical thresholds (PWMTs) before and 7 days after modeling. PWMT was assessed with the up-down method described previously,^{45,46} using a set of von Frey hairs with logarithmically incremental stiffness from 0.04 to 2.04 g (0.04, 0.07, 0.16, 0.4, 0.60, 1.0, 1.4, 2.04 g). The 0.4 g stimulus, in the middle of the series, was applied first. The observation of a positive response (paw lifting, shaking, or licking) within 5 seconds was then followed by an application of a thinner filament (or a thicker one if the response was negative).

Spared nerve injury (SNI) model

SNI surgeries were performed to mice according to previous works.^{22,23} In brief, mice were anesthetized with an injection of a mixture of chloral hydrate (0.4 g/kg ip). The skin of the lateral thigh was incised, and the biceps femoris muscle was dissected bluntly to expose the left sciatic nerve and its three terminal branches (the sural, common peroneal, and tibial nerves). The common peroneal and the tibial nerves were tightly ligated with 5-0 silk. Then, the nerve was transected distal to the ligation, and 2–4 mm length of nerve fiber was removed. Great care was taken to avoid any contact with or stretching of the intact sural nerve. The wound was closed in two layers. The Sham group was given all procedures except ligation.

Drug administration

Normal saline and minocycline were given intraperitoneally to mice in V-SNI and MC-SNI groups (Sigma-Aldrich Co., St Louis, MO, USA; 30 mg/kg), respectively, as scheduled: 16 and 1 h before surgery, then twice daily for 7 days after SNI.

RNA extraction

After the behavioral tests, the mice were sacrificed by rapid decapitation under anesthesia. After the exposure of the spinal cord with serial laminectomy, the lumbar (L4–L5) segments of spinal cords were transversely sectioned and hemi-dissected along the midline. Only the dorsal half of the lumbar spinal cord in the ipsilateral (operated) side of Sham, V-SNI and MC-SNI mice was collected, snap-frozen in liquid nitrogen, and stored at -80°C (193 K) until analysis. The tissue samples were washed three times with cold PBS and were scraped into Trizol reagent (Thermo Fisher Scientific, Waltham, MA, USA) according to the manufacturer's protocol. The quality and the concentration of the RNA samples were monitored at absorbance ratios of A260/A280 and A260/230 using a NanoDrop ND-1000 Spectrometer (NanoDrop Technologies, Wilmington, DE, USA). RNA integrity was assessed using standard denaturing agarose gel electrophoresis.

Microarray and computational analysis

The microarray hybridization and analysis were performed by Kangcheng Bio-tech, Shanghai PR China. Briefly, RNA was purified from total RNA after removal of rRNA (mRNA-ONLY Eukaryotic mRNA Isolation Kit, Epicentre). Then, each sample was amplified and transcribed into fluorescent cRNA along the entire length of the transcripts without 3' bias utilizing a random priming method. The labeled cRNAs were hybridized to the Mouse lncRNA Array v3.0 (8×60 K, Arraystar). About 35,923 lncRNAs and 24,881 coding transcripts which were collected from the most authoritative databases such as RefSeq, UCSC Knowngenes, Ensembl, and many related landmark publications can be detected. The arrays were scanned by the Agilent Scanner G2505B, and the acquired array images were analyzed by Agilent Feature Extraction software (version 11.0.1.1). Quantile normalization and subsequent data processing were performed by using the GeneSpring GX v12.1 software package (Agilent Technologies, Santa Clara, CA, USA). Normalized data were log₂-transformed and used for comparisons. lncRNAs and mRNAs, that is, at least 3 out of 9 samples have flags in

Present or Marginal (“All Targets Value”) were chosen for further data analysis. DE lncRNAs and mRNAs with statistical significance between the two groups were identified through *P*-value and fold change filtering.

qRT-PCR analysis

To verify the results of lncRNA microarray, reverse transcription was generated using the SuperScript™ III Reverse Transcriptase (Thermo Fisher Scientific) with a Gene Amp PCR System 9700 (Thermo Fisher Scientific). 1.5 μg RNA, 10 μM primer (Table 1), and 2.5 mM each deoxyribonucleotide triphosphates, were incubated for 5 minutes at 65°C and then chilled on ice for 2 minutes. 5× First Strand Buffer, 0.1 M DTT (final concentration), 0.3 μL RNase Inhibitor, and 0.2 μL Superscript III RT were then added. The 20 μL reaction was incubated for 60 minutes at 50°C followed by a final incubation at 70°C for 15 minutes for termination. Quantitative PCR was carried out on a real-time detection instrument ViiA 7 Real-time PCR System (Thermo Fisher Scientific) using 2× PCR master mix (Arraystar) at the following conditions: 10 minutes at 95°C , 40 cycles: 10 seconds at 95°C , and 60 seconds at 60°C . All the experiments were replicated three times. The relative expression of genes was calculated based on the $2^{-\Delta\Delta\text{Ct}}$ method using the mouse housekeeping GAPDH gene as an endogenous control.⁴⁷ Expression ratios were subjected to a log₂ transform to produce fold change data.

Functional annotation enrichment analysis

We used the Database for Annotation, Visualization and Integrated Discovery (DAVID) bioinformatics resources version 6.8^{48,49} (<https://david.ncifcrf.gov>) to perform GO (<http://www.geneontology.org>) analyses for mRNAs. The GO project provides a controlled vocabulary to describe gene and gene product attributes in any organism. The ontology covers three domains: biological process, cellular component, and molecular function. Kyoto Encyclopedia of Genes and Genomes (KEGG) pathway analysis is a functional analysis that maps genes to KEGG pathways. We applied a Fisher's

Table 1 The primers of 3 lncRNAs used in this study

lncRNA	Primer	Annealing temperature (°C)	Product length (bp)
NR_015491	F:5'TTGCTGAGCAGACTTGAATGA3' R:5'TTGCCTGAGCACAATCCACA3'	60	78
ENSMUST00000174263	F:5'CCCAGCATCAGGGTTTAGGA3' R:5'TCTCAGGGGATTTTCTTCTCTC3'	60	239
ENSMUST00000146263	F:5'GAGTCTCCCTGACCTAACCTG3' R:5'TGCCTTCTGTTCTTTGTGTTG3'	60	134

Abbreviation: lncRNA, long noncoding RNAs.

exact P -value cutoff <0.05 , correcting for multiple testing with the Benjamin's false discovery rate. Results of both the analyses were presented in enrichment score ($-\log_{10}(P\text{-value})$) sorted descending. Additionally, we used BinGO²⁶ plugin (v3.0.3) in Cytoscape (v3.4.0) to generate a P -value annotation tree, showing enrichments in related annotations.

Statistical analysis

All results were presented as mean \pm standard error. Statistical significance was determined by Student's t -test for 2 group comparison. Comparisons for 3 groups were conducted with analysis of variance and Turkey's correction. Both calculations were executed using GraphPad Prism software (version 6.0c). The threshold value used to screen DE lncRNAs and mRNAs was set fold change >2.0 . $P<0.05$ was considered statistically significant.

Results

Minocycline significantly attenuated neuropathic pain induced by SNI

Consistent with previous studies,^{22,23} the V-SNI group (which received repeated vehicle injections before and after SNI) showed a significant decrease in the PWMTs on the ipsilateral side on day 7, at 0.067 ± 0.035 g, when compared with the preoperative baseline values (3.191 ± 0.219 g, $P<0.0001$; Figure 1) and the values in the sham group (3.438 ± 0.192 g, $P<0.0001$; Figure 1). A significant attenuation in the PWMTs at 7 days after SNI was observed in the MC-SNI group (intraperitoneal [ip] administration of minocycline before and after SNI), at 0.554 ± 0.141 g, when compared to the V-SNI group ($P<0.001$). No significant difference was noted for the baseline PWMTs in the sham (3.438 ± 0.192 g), V-SNI (3.191 ± 0.211 g), and MC-SNI (2.913 ± 0.344 g) ($P>0.05$) groups.

Overview of lncRNA and mRNA expression profiles in the spinal cord after SNI and minocycline treatments

We used microarray technology to obtain an overall profile of lncRNA and mRNA expressions in the ipsilateral L4-L5 spinal cord. The expression features were displayed as scatter plots (Figure 2A–D). As shown in Figure 2A and B, a large number of DE lncRNAs and mRNAs were expressed in the V-SNI group compared to the sham group (1,200 DE lncRNAs and 739 DE mRNAs, fold change >2 , $P<0.05$), whereas the difference in the expression of DE lncRNAs and mRNAs was smaller between the V-SNI and MC-SNI groups (Figure 2C and D). Among these DE transcripts, 183 lncRNAs and 102 mRNAs were greatly altered (fold change >2 , $P<0.05$) in both the sham versus V-SNI and the V-SNI versus MC-SNI groups. These data suggest that SNI led to a substantial alteration in gene expression of lncRNAs and mRNAs, whereas the use of minocycline caused only a slight alteration.

The DE transcripts between the sham and V-SNI groups aided in the filtering of lncRNAs and mRNAs that were altered following SNI. The comparison between the V-SNI and MC-SNI groups aided in filtering genes that were DE due to minocycline. The results from these three groups, when taken together, enabled a more accurate identification of genes associated with SNI-induced neuropathic pain.

Gene regulation under two different circumstances was evaluated by dividing the DE genes into two major expression patterns: A and B. Pattern A included genes that were modulated only by SNI, whereas pattern B represented genes that were modulated by both SNI and repeated minocycline administration. Specifically, B1 represented genes that were upregulated by SNI and then downregulated by minocycline; B2 genes were those downregulated by SNI and then

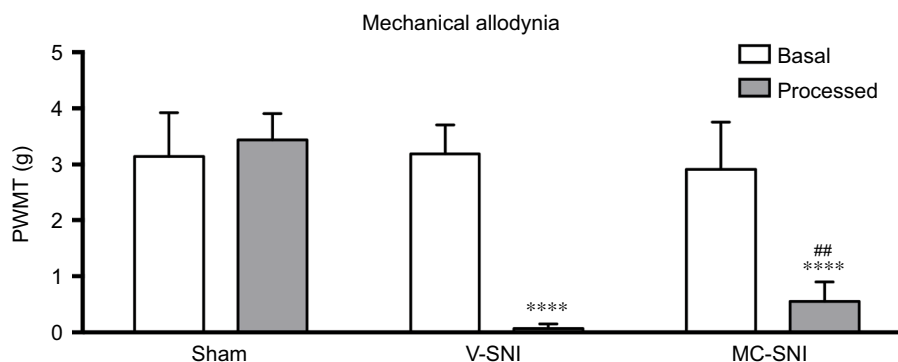


Figure 1 The paw withdrawal mechanical thresholds (PWMTs) at baseline and 7 days after modeling are presented as mean \pm standard error ($n=6$). **** $P<0.0001$ indicates a statistically significant difference when compared to its baseline and Sham group and ### $P<0.001$ indicates a statistically significant difference when compared to the V-SNI group.

Abbreviations: MC-SNI, group that had minocycline repeatedly administered before and after SNI; PWMT, paw withdrawal mechanical threshold; SNI, spared nerve injury; V-SNI, group that repeated vehicle injections before and after SNI.

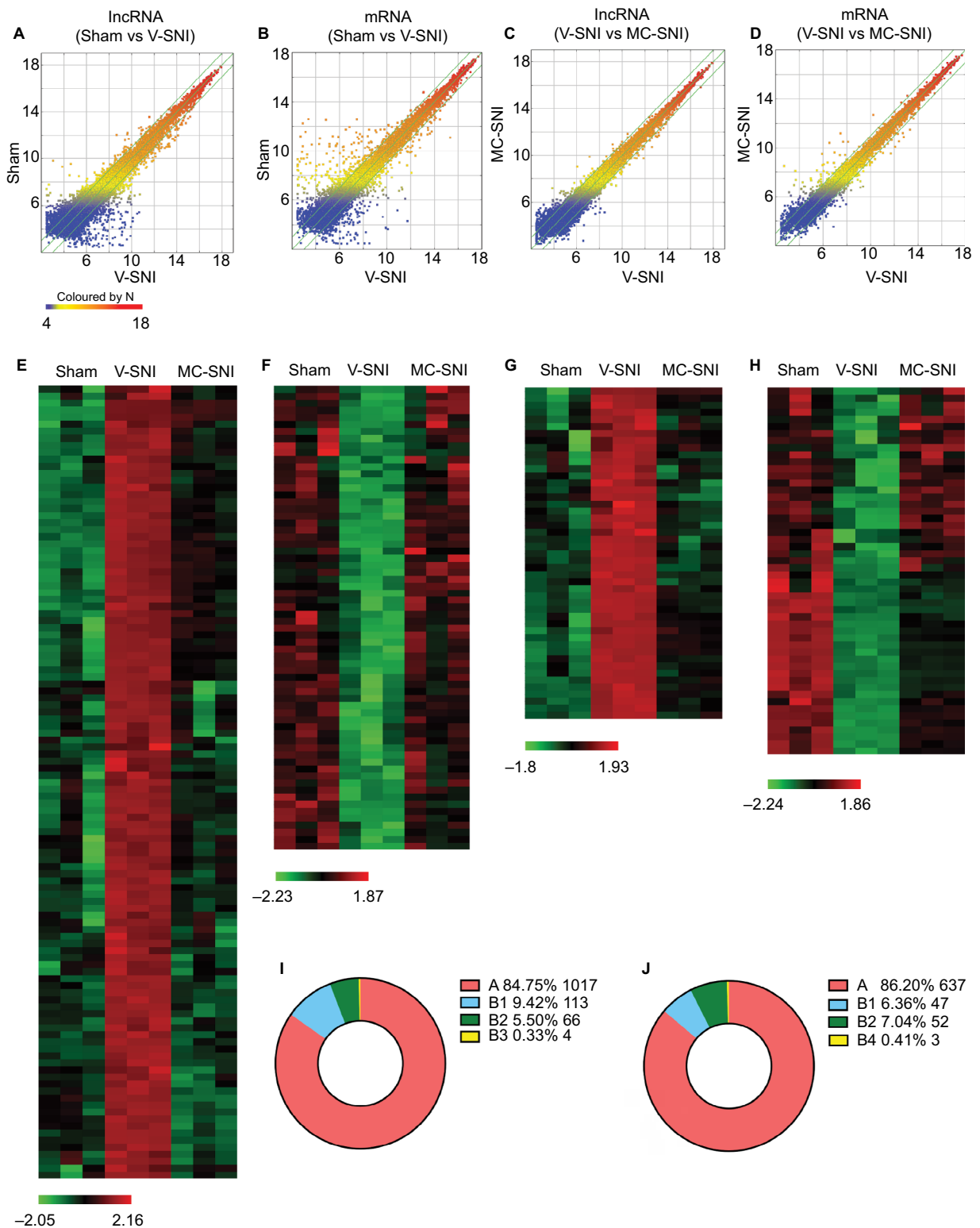


Figure 2 Scatter plots compare the expression of lncRNAs and mRNAs between the sham versus V-SNI group (A and B), and V-SNI versus MC-SNI group (C and D). The values of X and Y axes in the scatter plot are the averaged normalized values in each group (log₂ scaled). The green lines indicate a fold change value of 2.0. The transcripts above the top green line and below the bottom green line indicate more than 2-fold changes between pairs. In total, 113 lncRNAs in B1 and 66 in B2 were listed in heat maps E and F; and 47 mRNAs in B1 and 52 in B2 were listed in heat maps G and H. In the heat maps, each column represents a microarray group, while each row represents a regulated gene. The color scale illustrates the relative expression level of lncRNAs: red denotes rich abundance and green denotes poor abundance. Percentages of each pattern for lncRNAs and mRNAs were shown in donut charts (I and J). Pattern A included genes that were modulated only by SNI, whereas pattern B represented genes that were modulated by both SNI and repeated minocycline administration. B1 - genes upregulated by SNI and then downregulated by minocycline, B2 - genes downregulated by SNI and then upregulated by minocycline, B3 - genes upregulated by SNI and further upregulated by minocycline, and B4 - genes downregulated by SNI and further downregulated by minocycline. **Abbreviations:** lncRNA, long noncoding RNA; MC-SNI, group that had minocycline repeatedly administered before and after SNI; SNI, spared nerve injury; V-SNI, group that repeated vehicle injections before and after SNI.

upregulated by minocycline; B3 genes were upregulated by SNI and further upregulated by minocycline, and B4 genes were downregulated by SNI and further downregulated by minocycline.

Behavioral tests indicated that minocycline had an alleviating effect on the PWMTs, suggesting that it partially counteracted the effects of SNI. Genes that had an adverse effect on regulation (patterns B1 and B2) could be more responsible for this effect. The gene classification identified 1,017 lncRNAs in pattern A, 113 in B1, 66 in B2, and 4 in B3. The heat maps of DE lncRNAs in B1 and B2 are shown in Figure 2E and F, respectively.

Among the 739 DE mRNAs detected after SNI, 102 mRNAs were modulated by repeated minocycline administration and were categorized based on the four B-type expression patterns. In total, 47 mRNAs were classified as B1, 52 as B2, and 3 as B4. The levels of the remaining 637 mRNAs were not modulated by minocycline (pattern A). The heat maps of DE mRNAs for the B1 and B2 mRNAs are shown in Figure 2G and H, respectively. The pattern distribution for lncRNAs and mRNAs are shown in Figure 2I and 2J, respectively.

Quantitative real-time polymerase chain reaction (qRT-PCR) validation of 3 lncRNAs

The reliability of the microarray results was validated by qRT-PCR analysis of lncRNAs *NR_015491*, *ENSMUST00000174263*, and *ENSMUST00000146263*.

NR_015491

In the spinal cord, an upregulation of *NR_015491* (1.00 ± 0.22 vs 2.06 ± 0.07 , $P < 0.01$) was observed 7 days after SNI. Minocycline significantly diminished the level of *NR_015491* by 0.67 ± 0.08 ($P < 0.001$, Figure 3A). The qRT-PCR analyses confirmed the changes detected by the microarray. The quantity of *NR_015491* was upregulated by 3.75 ± 0.43 ($P < 0.01$) and downregulated by 2.22 ± 0.33 ($P < 0.05$) in the MC-SNI group (Figure 3B).

ENSMUST00000174263

The microarray results indicated a fold change increase of 3.99 ± 0.09 ($P < 0.0001$) in V-SNI group and a decrease of 1.23 ± 0.18 in the MC-SNI group ($P < 0.0001$; Figure 3C).

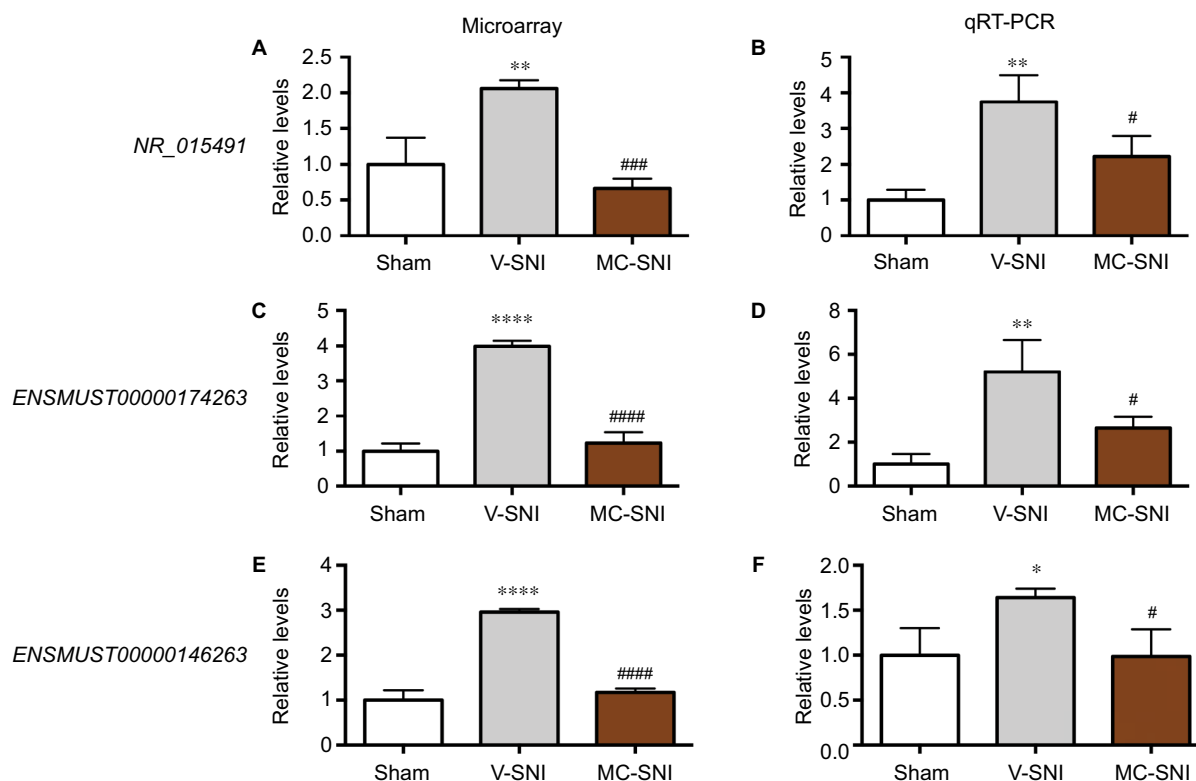


Figure 3 The fold changes of the detected lncRNAs *NR_015491*, *ENSMUST00000174263*, and *ENSMUST00000146263* using microarray (**A**, **C**, and **E**) and qRT-PCR (**B**, **D**, and **F**) were listed. The statistical analysis for each comparison was performed using ANOVA and Turkey's correction. * $P < 0.05$, ** $P < 0.01$, and **** $P < 0.0001$ indicate a statistically significant difference when compared to the sham group; # $P < 0.05$, #### $P < 0.001$, and ##### $P < 0.0001$ indicate a significant difference when compared to V-SNI.

Abbreviations: ANOVA, analysis of variance; lncRNA, long noncoding RNA; MC-SNI, group that had minocycline repeatedly administered before and after SNI; qRT-PCR, quantitative real-time polymerase chain reaction; SNI, spared nerve injury; V-SNI, group that repeated vehicle injections before and after SNI.

The qRT-PCR analyses indicated a fold change increase in *ENSMUST00000174263* by 5.21 ± 0.84 ($P < 0.01$) in the V-SNI group and a decrease of 2.66 ± 0.30 ($P < 0.05$) in the MC-SNI group (Figure 3D), in agreement with the microarray data.

ENSMUST00000146263

The microarray analyses indicated a fold change increase in the V-SNI group (from 1.00 ± 0.12 to 2.96 ± 0.04 , $P < 0.0001$) and a fold decrease of 1.17 ± 0.04 in the MC-SNI group ($P < 0.0001$; Figure 3E). The qRT-PCR analysis indicated a fold increase for *ENSMUST00000146263* of 1.64 ± 0.06 ($P < 0.05$) in the V-SNI group and a fold decrease of 0.99 ± 0.17 ($P < 0.05$) in the MC-SNI group (Figure 3F), confirming microarray data.

Class distribution analyses of DE lncRNAs

The DE lncRNAs were classified into 4 categories based on their genomic proximity to protein-coding genes:^{24,25} 1) intergenic lncRNAs (lincRNAs), 2) bidirectional lncRNAs, 3) sense lncRNAs, and 4) antisense lncRNAs. The lincRNAs are found in regions that are free of other genes. The bidirectional lncRNAs are oriented head-to-tail to a coding transcript within 1 kb. The sense lncRNAs are transcribed from the sense strand of protein-coding genes and contain exons from protein-coding genes; they may overlap with part of the protein-coding genes or cover the entire sequence of the protein-coding gene. Antisense lncRNAs, by contrast, are transcribed from the antisense strand of protein-coding genes. As shown in Figure 4, lincRNAs

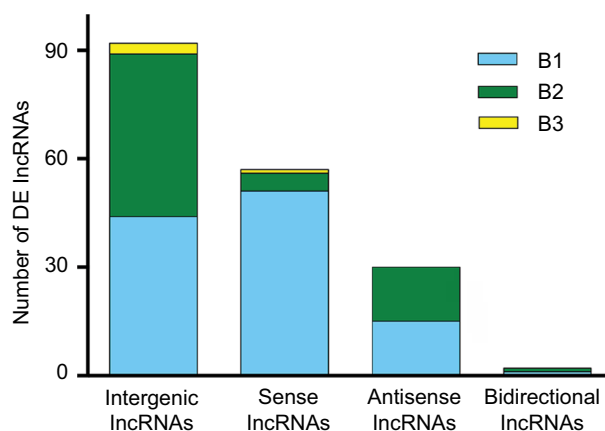


Figure 4 Distribution of four lncRNA classes. The distribution of intergenic, sense, antisense, and bidirectional lncRNAs is identified. Blue, green, and yellow colors indicate the number of DE lncRNAs with expression pattern B1, B2, or B3 in each class. Pattern B represented genes that were modulated by both SNI and repeated minocycline administration. B1 - genes upregulated by SNI and then downregulated by minocycline, B2 - genes downregulated by SNI and then upregulated by minocycline, and B3 - genes upregulated by SNI and further upregulated by minocycline.

Abbreviations: DE, differentially expressed; lncRNA, long noncoding RNA.

accounted for most of the 183 DE lncRNAs modulated by both SNI and minocycline (pattern B): we identified 92 lincRNAs, 59 sense lncRNAs, 30 antisense lncRNAs, and 2 bidirectional lncRNAs.

Functional prediction of DE mRNAs

We explored the possible biological functions that were altered after SNI by focusing on the 739 DE mRNAs identified by comparing the sham and V-SNI groups. The expressions of 390 mRNAs were upregulated ($P < 0.05$, fold change > 2.0), and the remaining 349 were downregulated ($P < 0.05$, fold change > 2.0). Performance of gene ontology (GO) and the KEGG pathway analyses showed that chemokine activity, chemokine receptor binding, and cytokine activity were among the most enriched GO molecular function annotations of the upregulated mRNAs (Figure 5A; Table 2). A *P*-value annotation tree was generated using the BinGO²⁶ plugin in Cytoscape with these mRNAs. Part of the tree, shown in Figure 5B, revealed a relationship between the ending annotation nodes, like chemokine activity, as well as the abundant enrichment of their parent annotations (eg. protein binding, receptor binding, and growth factor binding), indicating a concentrative functional change at the gene level.

The transcripts that showed obvious dysregulation by SNI and minocycline (fold change > 2 in both the circumstances), which might more strongly reflect a minocycline effect, were also enriched in the GO and KEGG annotations. These transcripts were mainly attributed to the application of minocycline and therefore attracted our interest the most. The paucity of DE mRNAs identified between the V-SNI and MC-SNI groups prompted the inclusion of the genomic proximity-related mRNAs of the DE lncRNAs (V-SNI vs MC-SNI) in the analysis.

Actin binding, serine-type endopeptidase, and hydrolyase activities were among the most enriched molecular function annotations (Figure 5C; Table 3). Osteoblast proliferation, myofibril assembly, muscle contraction, and glucose and insulin processes were positively regulated and were the most enriched biological process annotations (Figure 5D).

Discussion

Very few studies have focused on neuropathic pain and lncRNAs, despite the strong scientific interest in lncRNAs. To our knowledge, this is the first study to identify global expression changes in lncRNAs in the spinal cord following SNI and minocycline treatment and to explore the possible mechanisms underlying neuropathic pain.

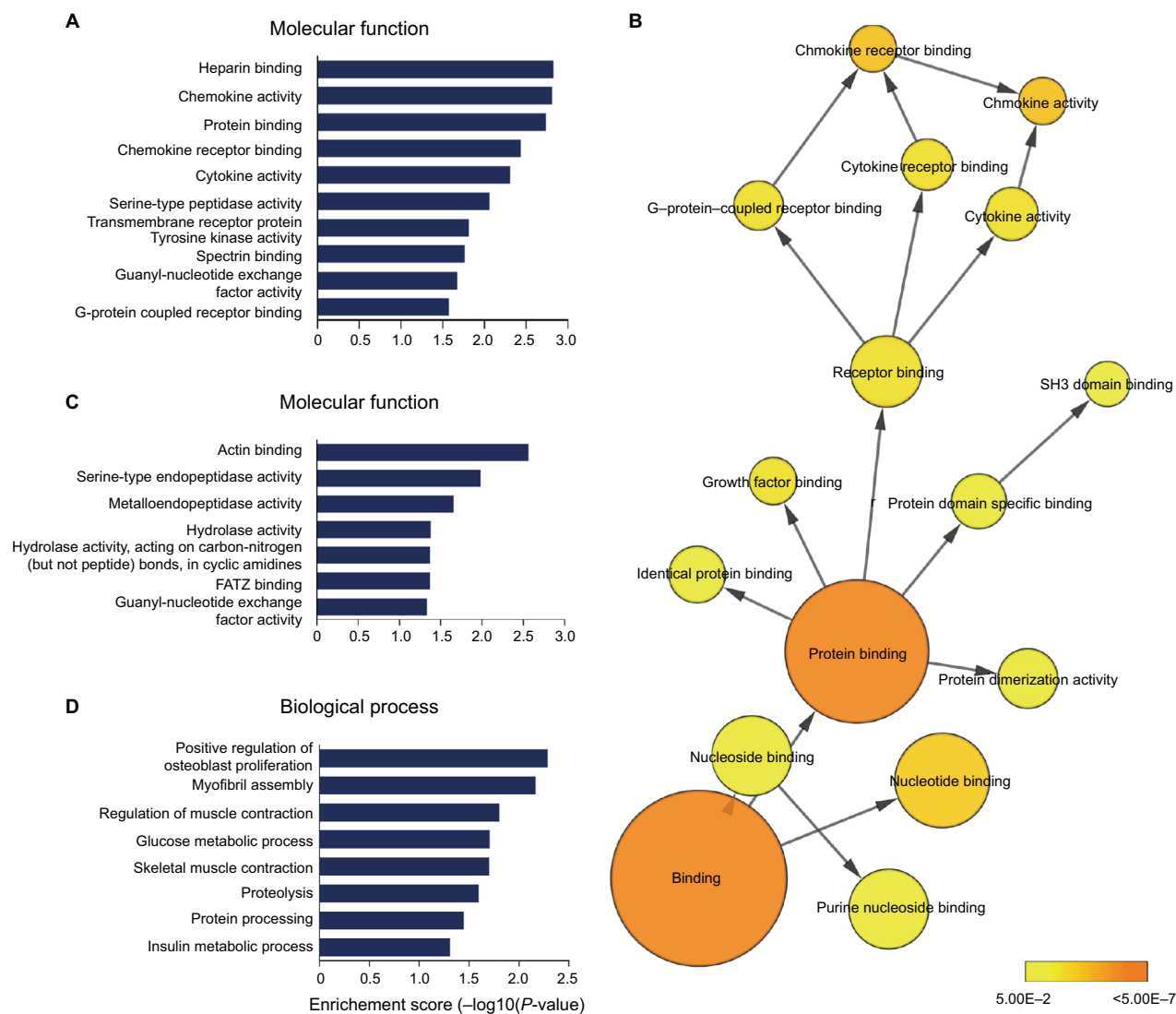


Figure 5 (A) The enriched molecular function annotations for DE mRNAs from sham versus V-SNI groups. (B) Part of the P-value annotation tree was displayed to reveal chemokine activity and its greatly enriched related annotations. (C and D) The enriched molecular function and biological process annotations for DE mRNAs from V-SNI versus MC-SNI. GO results are presented as descending enrichment scores.

Abbreviations: DE, differentially expressed; GO, gene ontology; MC-SNI, group that had minocycline repeatedly administered before and after SNI; SNI, spared nerve injury; V-SNI, group that repeated vehicle injections before and after SNI.

Behavioral tests, performed on all mice before modeling and sampling, confirmed previous findings^{22,23} that minocycline alleviates SNI-induced allodynia (Figure 1). Microarray analysis identified 183 lncRNAs and 102 mRNAs that could represent potential therapeutic targets for minocycline (Figure 2). The qRT-PCR analysis showed changes in expression levels of *NR_015491*, *ENSMUST00000174263*, and *ENSMUST00000146263* that were consistent with the microarray results (Figure 3), thereby validating the microarray data. Similarly, Jiang et al reported 511 DE (fold change >2) lncRNAs (366 upregulated and 145 downregulated) in a spinal nerve ligation-induced neuropathic pain model.¹⁴ Therefore, lncRNAs may be involved in neuropathic pain processing.

The vast majority of lncRNA functions are unclear, but emerging evidence now suggests that some lncRNAs play critical roles in neuropathic pain. For example, the lncRNA *NONRATT021972*, a small interfering RNA, may suppress the upregulation of the P2X₃ receptor to reduce the hyperalgesia potentiated by the proinflammatory cytokine TNF- α in type 2 diabetes mellitus rats.¹⁷ This lncRNA may also decrease the expression levels of P2X₇ mRNA and protein, inhibit the activation of satellite glial cells, and reduce the release of TNF- α , thereby inhibiting the excitability of DRG neurons and decreasing mechanical and thermal hyperalgesia in these rats.¹⁸ An antisense lncRNA, *Kcna2*, is also associated with excitability in DRG neurons through modulation of the Kv current.¹⁵ The lncRNA *uc.48+*, another small inter-

Table 2 Molecular function annotation enrichment results comparing sham versus V-SNI

No.	Term	P-value	Genes
1	Heparin binding	0.001499866	VEGFB, FGFR4, CCL2, NAV2, CCL5, CCL7, ITGAM, ABI3BP, CXCL10, CYR61
2	Chemokine activity	0.001548949	CCL2, CCL19, CCL5, CXCL12, CCL7, CXCL10
3	Protein binding	0.001837527	PRX, SGSH, RHOJ, HSP90AB1, APOBEC3, HPS5, CLSTN3, USH1G, PAX6, RHOQ, ANKRD1, JAG1, CXADR, CD96, NOD1, CD44, RAVR2, ANK3, HOMER3, ATG7, SERPINE1, SPG20, ANO2, PIK3API, PILRA, EGFR, DYNC111, RBFOX2, SH3PXD2A, LYN, CCDC88C, RXRB, FMR1, ZFP467, SIX3, PDXP, BICD2, PPARGC1B, PDCD1LG2, CARD11, ARVCF, DSG1A, CD36, ZFAND2B, ROR2, H2-AA, VGLL2, FLII, CD226, CD300LD, ABCA7, FGFR4, NKD1, IL1R1, CCL2, RAB3D, PRTN3, CD247, CNTFR, CHEK1, ITGB2, BCL2L2, PAXBPI, CBLL1, TCF7L2, CTLA2B, MOV10, STAT4, GFII, NFATC2, TCF3, PXT1, LRFN2, HAVCR2, FYB, EIF4ENIF1, CR2, TRNPI, TGFB2, EN1, DOCK7, AMBRA1, IDO1, HSI3BP3, VAV1, PPP1R3L, DVLI, SYNE3, EPHA4, LCE1G, EPS8, CMYA5, CYFIP2, MILR1, CIT, BMPR1B
4	Chemokine receptor binding	0.003686081	CCL19, CCL5, S100A14, CXCL12
5	Cytokine activity	0.004934124	IL17A, CCL2, CIQTNF4, IFNE, IL17F, TNFSF12, INHA, CCL5, CXCL12, CCL7, CXCL10
6	Serine-type peptidase activity	0.008639921	TMPRSS11G, PRTN3, CFB, CTRB1, TYSND1, DPP8, CFI, TMPRSS12, HABP2
7	Transmembrane receptor protein tyrosine kinase activity	0.015247211	EGFR, EPHA4, FGFR4, LTK, ROR2
8	Spectrin binding	0.017147753	DYNC111, DMTN, ANK3, USH1G
9	Guanyl-nucleotide exchange factor activity	0.021272918	FGD2, DOCK2, CYTH4, PSD4, DOCK7, VAV1, EIF2B3, RGL1
10	G-protein-coupled receptor binding	0.026730704	GNA14, GNA15, CCL2, DNAJC14, USP20
11	RNA polymerase II core promoter proximal region sequence-specific DNA binding	0.027051751	PAX6, ZFP467, EN1, PAXBPI, FOSB, TCF7L2, FEZF2, SMARCD2, PRDM5, ZFP219, NFATC2, TCF3, NFIA
12	Transcriptional repressor activity, RNA polymerase II core promoter proximal region sequence-specific binding	0.027375039	STAT6, PRDM5, ZFP219, EN1, GFII, NFATC2, TCF3
13	Integrin binding	0.032537287	EGFR, LYN, ITGA2, CXADR, CD226, CYR61
14	Serine-type endopeptidase activity	0.035490515	TMPRSS11G, F5, PRTN3, CFB, CTRB1, TYSND1, CFI, TMPRSS12, HABP2
15	GTP binding	0.040618394	HSP90AB1, RHOJ, GNA14, GNA15, RAB3D, TUBA3B, RHOQ, RAB40C, NPR2, I70009NI4RIK, RND1, TUBB6, NKIRAS2

Abbreviations: SNI, spared nerve injury; V-SNI, group that repeated vehicle injections before and after SNI.

Table 3 Molecular function annotation enrichment results comparing V-SNI versus MC-SNI

No.	Term	P-value	Genes
1	Actin binding	0.002751885	TNNT3, TRIOBP, SHROOM3, TNNC2, SYNPO2, MYOZ1, MYOZ2, TPM4, FLNA, TNNI2
2	Serine-type endopeptidase activity	0.010409829	MMP8, GM2663, LTF, 2210010C04RIK, MCPT2, TMPRSS12, CTSG
3	Metalloendopeptidase activity	0.022158153	ADAM28, ADAMTS9, ADAM29, MMP8, PMPCB
4	Hydrolase activity	0.041880873	APOBEC2, ADAM28, APOBEC3, CPPED1, PTPRN2, MMP8, PTPN14, PGAM2, MCPT2, MTMR2, NT5C3, PLA2G12A, ACOT11, VPS4B, ATP8B1, PARG, LTF, TMPRSS12, HDAC8, CTSG, PMPCB
5	FATZ binding	0.042538506	APOBEC2, APOBEC3
6	Hydrolase activity, acting on carbon-nitrogen (but not peptide) bonds, in cyclic amidines	0.042538506	MYOZ1, MYOZ2
7	Guanyl-nucleotide exchange factor activity	0.046446397	FGD2, DENND5A, RARF6, DOCK7, DENND4B
8	Metallopeptidase activity	0.050491587	ADAM28, ADAMTS9, ADAM29, MMP8, PMPCB
9	Telethonin binding	0.050827978	MYOZ1, MYOZ2
10	Catalytic activity	0.056869731	APOBEC2, XDH, APOBEC3, SPTLC2, CKMT2, ABAT, PGAM2, PCYT1B, PMPCB

Abbreviations: MC-SNI, group that had minocycline repeatedly administered before and after SNI; SNI, spared nerve injury; V-SNI, group that repeated vehicle injections before and after SNI.

fering RNA, may alleviate DNP by inhibiting the excitatory transmission mediated by the P2X₃ receptor in the DRG.¹⁶ Further studies are needed to confirm the roles of these DE lncRNAs in neuropathic pain.

Most DE lncRNAs with pattern B were categorized as intergenic (Figure 4), as they arise from genomic loci that are located far from other annotated genes.²⁷ These lincRNAs tend to affect the expression of their neighboring

genes through different types of mechanisms.^{27–29} However, in the present case, none of the neighboring or overlapping protein-coding genes were simultaneously altered, indicating that posttranscriptional or translational interference might be more responsible for the regulation.

In our study, we also examined the expression profile of mRNAs by microarrays. Bioinformatics analyses for mRNAs upregulated after SNI showed that a large number of molecular functions of the affected genes were implicated in cytokine and chemokine activities (Figure 5A). Pro-nociceptive factors released from neurons and non-neuronal cells are known to sensitize the neuron of the first pain synapse³⁰ and mediate multistep responses to counteract foreign insults; hence, they play vital roles in the development and maintenance of chronic pain.^{31,32} Our microarray analysis revealed two cytokine protein-coding transcripts (IL17A and IL17F) among the significantly upregulated mRNAs. Furthermore, a number of CC and CXC chemokine transcripts (eg, CCL2, CCL5, CCL7, CXCL10, and CXCL12) were also identified (Table 2). These results supported the classical theory that cytokine and chemokine dysregulations are involved in neuropathic pain through the enhancement of nociceptive transmission.

Minocycline, as an effective pain alleviator, was employed as a treatment control to allow us to filter transcripts that were more related to neuropathic pain. Its use also allowed us to further explore its exact mechanisms. The DE lncRNAs and mRNAs with pattern B were apparently most related to the genomic regulatory functions of this drug. Bioinformatics analysis demonstrated an enrichment of minocycline-induced DE mRNAs with pattern B and that these had molecular function annotations in actin-binding and intracellular enzyme activities (Figure 4C). Thus, minocycline might exert its effects by regulating actin functions at the gene level. Actin binding is believed to regulate spine morphology and synaptic function through the cytoskeleton,^{33,34} thereby controlling nociception function.³⁵ A previous study³⁶ addressed the link between impairment of microtubule dynamics and synaptic plasticity in the spinal dorsal horn and the occurrence of paclitaxel-induced painful neuropathy. Pregabalin weakened the formation of web-like filamentous actin (F-actin) and affected cytoskeleton proteins,³⁷ suggesting that chronic pain was associated with changes in the cytoskeleton array and protein folding. The RhoA/LIMK/cofilin pathway is known to modulate the levels of F-actin³⁸ and control the stabilization of actin cytoskeleton. Neurite outgrowth is

closely connected to modulations of the cytoskeleton, and microtubule and actin dynamics in particular;³⁹ therefore, actin-binding activity may be pivotal in these regulations. Our microarray analysis detected statistically significant modulation of *LIMK1* mRNA, but the fold changes were not >2. Nevertheless, these results supported the possibility of minocycline regulation of actin functions.

Bioinformatics prediction provides a first glance at the functions of the DE mRNAs. However, the limited evidence precluded establishment of the actual role of minocycline, and several limitations should be considered when interpreting our results. First, we used bioinformatics methods solely to predict the possible biological functions that DE mRNAs might participate in. Subsequent studies based on this work might use other methods to validate the possible pathways involved. Second, we sampled spinal dorsal horn tissue only, as this is a site of interest to us in our research. Nevertheless, other areas in the CNS are related to neuropathic pain (eg, the anterior cingulate cortex,⁴⁰ the ventral tegmental area,⁴¹ and the mesencephalic periaqueductal gray^{42,43}). Further studies might include these other areas and compare the identified lncRNAs with the ones from this work. Taken together, the results from the present work have revealed SNI- and minocycline-induced gene alterations, which might provide new verification of the role for lncRNAs as crucial mediators and potential therapeutic targets for the treatment of neuropathic pain.

Conclusion

In summary, microarray technology allowed us to identify and study DE lncRNAs and mRNAs associated with SNI-induced neuropathic pain. SNI-induced gene regulations might be involved in cytokine (IL17A and IL17F) and chemokine (CCL2, CCL5, and CCL7) activities. Minocycline might exert its pain-alleviating effect on mice through actin binding, thereby regulating nociception via control of the cytoskeleton. In the near future, ongoing research is expected to elucidate the roles of individual lncRNAs. Collectively, the results of the present study provide a first step toward future research into effective and safe genetic therapies for the treatment of neuropathic pain.

Acknowledgments

This work was supported by grants from the National Natural Science Foundation of China (number 31100805) and the Project of Science and Technology New Star in Zhujiang Guangzhou City (number 2012J2200036).

Disclosure

The authors report no conflicts of interest in this work.

References

- Gilron I, Baron R, Jensen T. Neuropathic pain: principles of diagnosis and treatment. *Mayo Clin Proc.* 2015;90(4):532–545.
- Jensen TS, Baron R, Haanpaa M, et al. A new definition of neuropathic pain. *Pain.* 2011;152(10):2204–2205.
- von Hehn CA, Baron R, Woolf CJ. Deconstructing the neuropathic pain phenotype to reveal neural mechanisms. *Neuron.* 2012;73(4):638–652.
- Woolf CJ. Central sensitization: implications for the diagnosis and treatment of pain. *Pain.* 2011;152(3 Suppl):S2–S15.
- Watkins LR, Milligan ED, Maier SF. Spinal cord glia: new players in pain. *Pain.* 2001;93(3):201–205.
- Watkins LR, Milligan ED, Maier SF. Glial activation: a driving force for pathological pain. *Trends Neurosci.* 2001;24(8):450–455.
- Watkins LR, Maier SF. Glia: a novel drug discovery target for clinical pain. *Nat Rev Drug Discov.* 2003;2(12):973–985.
- Liang F, Holt I, Perteua G, Karamycheva S, Salzberg SL, Quackenbush J. Gene index analysis of the human genome estimates approximately 120,000 genes. *Nat Genet.* 2000;25(2):239–240.
- Costa FF. Non-coding RNAs: meet thy masters. *Bioessays.* 2010;32(7):599–608.
- Qureshi IA, Mehler MF. Long non-coding RNAs: novel targets for nervous system disease diagnosis and therapy. *Neurotherapeutics.* 2013;10(4):632–646.
- Batista PJ, Chang HY. Long noncoding RNAs: cellular address codes in development and disease. *Cell.* 2013;152(6):1298–1307.
- Lipovich L, Tarca AL, Cai J, et al. Developmental changes in the transcriptome of human cerebral cortex tissue: long noncoding RNA transcripts. *Cereb Cortex.* 2014;24(6):1451–1459.
- Ponjavic J, Oliver PL, Lunter G, Ponting CP. Genomic and transcriptional co-localization of protein-coding and long non-coding RNA pairs in the developing brain. *PLoS Genet.* 2009;5(8):e1000617.
- Jiang BC, Sun WX, He LN, Cao DL, Zhang ZJ, Gao YJ. Identification of lncRNA expression profile in the spinal cord of mice following spinal nerve ligation-induced neuropathic pain. *Mol Pain.* 2015;11:43.
- Zhao X, Tang Z, Zhang H, et al. A long noncoding RNA contributes to neuropathic pain by silencing Kcna2 in primary afferent neurons. *Nat Neurosci.* 2013;16(8):1024–1031.
- Wang S, Xu H, Zou L, et al. LncRNA uc.48+ is involved in diabetic neuropathic pain mediated by the P2X3 receptor in the dorsal root ganglia. *Purinergic Signal.* 2016;12(1):139–148.
- Peng H, Zou L, Xie J, et al. LncRNA NONRATT021972 siRNA decreases diabetic neuropathic pain mediated by the P2X3 receptor in dorsal root ganglia. *Mol Neurobiol.* 2017;54(1):511–523.
- Liu S, Zou L, Xie J, et al. LncRNA NONRATT021972 siRNA regulates neuropathic pain behaviors in type 2 diabetic rats through the P2X7 receptor in dorsal root ganglia. *Mol Brain.* 2016;9:44.
- Moller T, Bard F, Bhattacharya A, et al. Critical data-based re-evaluation of minocycline as a putative specific microglia inhibitor. *Glia.* 2016;64(10):1788–1794.
- Zemke D, Majid A. The potential of minocycline for neuroprotection in human neurologic disease. *Clin Neuropharmacol.* 2004;27(6):293–298.
- Sumitani M, Ueda H, Hozumi J, et al. Minocycline does not decrease intensity of neuropathic pain intensity, but does improve its affective dimension. *J Pain Palliat Care Pharmacother.* 2016;30(1):31–35.
- Richner M, Bjerrum OJ, Nykjaer A, Vaegter CB. The spared nerve injury (SNI) model of induced mechanical allodynia in mice. *J Vis Exp.* 2011;(54):pii:3092.
- Decosterd I, Woolf CJ. Spared nerve injury: an animal model of persistent peripheral neuropathic pain. *Pain.* 2000;87(2):149–158.
- Ma L, Bajic VB, Zhang Z. On the classification of long non-coding RNAs. *RNA Biol.* 2013;10(6):924–933.
- Ponting CP, Oliver PL, Reik W. Evolution and functions of long noncoding RNAs. *Cell.* 2009;136(4):629–641.
- Maere S, Heymans K, Kuiper M. BiNGO: a cytoscape plugin to assess overrepresentation of gene ontology categories in biological networks. *Bioinformatics.* 2005;21(16):3448–3449.
- Ulitsky I, Bartel DP. lincRNAs: genomics, evolution, and mechanisms. *Cell.* 2013;154(1):26–46.
- Rinn JL, Chang HY. Genome regulation by long noncoding RNAs. *Annu Rev Biochem.* 2012;81:145–166.
- Mattick JS, Rinn JL. Discovery and annotation of long noncoding RNAs. *Nat Struct Mol Biol.* 2015;22(1):5–7.
- Clark AK, Old EA, Malcangio M. Neuropathic pain and cytokines: current perspectives. *J Pain Res.* 2013;6:803–814.
- Ji RR, Xu ZZ, Gao YJ. Emerging targets in neuroinflammation-driven chronic pain. *Nat Rev Drug Discov.* 2014;13(7):533–548.
- Zhang ZJ, Cao DL, Zhang X, Ji RR, Gao YJ. Chemokine contribution to neuropathic pain: respective induction of CXCL1 and CXCR2 in spinal cord astrocytes and neurons. *Pain.* 2013;154(10):2185–2197.
- Ethell IM, Pasquale EB. Molecular mechanisms of dendritic spine development and remodeling. *Prog Neurobiol.* 2005;75(3):161–205.
- Cingolani LA, Goda Y. Actin in action: the interplay between the actin cytoskeleton and synaptic efficacy. *Nat Rev Neurosci.* 2008;9(5):344–356.
- Woolf CJ, Salter MW. Neuronal plasticity: increasing the gain in pain. *Science.* 2000;288(5472):1765–1769.
- Chen SR, Zhu L, Chen H, Wen L, Laumet G, Pan HL. Increased spinal cord Na(+)-K(+)-2Cl(-) cotransporter-1 (NKCC1) activity contributes to impairment of synaptic inhibition in paclitaxel-induced neuropathic pain. *J Biol Chem.* 2014;289(45):31111–31120.
- Park S, Lee J. Proteomic analysis to identify early molecular targets of pregabalin in C6 glial cells. *Cell Biol Int.* 2009;34(1):27–33.
- Maekawa M, Ishizaki T, Boku S, et al. Signaling from Rho to the actin cytoskeleton through protein kinases ROCK and LIM-kinase. *Science.* 1999;285(5429):895–898.
- Zulauf L, Coste O, Marian C, Moser C, Brenneis C, Niederberger E. Cofilin phosphorylation is involved in nitric oxide/cGMP-mediated nociception. *Biochem Biophys Res Commun.* 2009;390(4):1408–1413.
- Johansen JP, Fields HL, Manning BH. The affective component of pain in rodents: direct evidence for a contribution of the anterior cingulate cortex. *Proc Natl Acad Sci U S A.* 2001;98(14):8077–8082.
- Ozaki S, Narita M, Narita M, et al. Suppression of the morphine-induced rewarding effect in the rat with neuropathic pain: implication of the reduction in mu-opioid receptor functions in the ventral tegmental area. *J Neurochem.* 2002;82(5):1192–1198.
- Rodriguez-Munoz M, Sanchez-Blazquez P, Vicente-Sanchez A, Berrocoso E, Garzon J. The mu-opioid receptor and the NMDA receptor associate in PAG neurons: implications in pain control. *Neuropsychopharmacology.* 2012;37(2):338–349.
- Owen SL, Green AL, Nandi DD, Bittar RG, Wang S, Aziz TZ. Deep brain stimulation for neuropathic pain. *Acta Neurochir Suppl.* 2007;97(Pt 2):111–116.
- Zimmermann M. Ethical guidelines for investigations of experimental pain in conscious animals. *Pain.* 1983;16(2):109–110.
- Chaplan SR, Bach FW, Pogrel JW, Chung JM, Yaksh TL. Quantitative assessment of tactile allodynia in the rat paw. *J Neurosci Methods.* 1994;53(1):55–63.
- Dixon WJ. Efficient analysis of experimental observations. *Annu Rev Pharmacol Toxicol.* 1980;20:441–462.
- Livak KJ, Schmittgen TD. Analysis of relative gene expression data using real-time quantitative PCR and the 2(-Delta Delta C(T)) Method. *Methods.* 2001;25(4):402–408.
- Huang da W, Sherman BT, Lempicki RA. Systematic and integrative analysis of large gene lists using DAVID bioinformatics resources. *Nat Protoc.* 2009;4(1):44–57.
- Huang da W, Sherman BT, Lempicki RA. Bioinformatics enrichment tools: paths toward the comprehensive functional analysis of large gene lists. *Nucleic Acids Res.* 2009;37(1):1–13.

Journal of Pain Research

Dovepress

Publish your work in this journal

The Journal of Pain Research is an international, peer reviewed, open access, online journal that welcomes laboratory and clinical findings in the fields of pain research and the prevention and management of pain. Original research, reviews, symposium reports, hypothesis formation and commentaries are all considered for publication.

The manuscript management system is completely online and includes a very quick and fair peer-review system, which is all easy to use. Visit <http://www.dovepress.com/testimonials.php> to read real quotes from published authors.

Submit your manuscript here: <https://www.dovepress.com/journal-of-pain-research-journal>